Experimental Validation of Monte Carlo Dose Calculation System for Interventional Radiology

Sungho Moon[a], Haegin Han[a], Gahee Son[a], Chansoo Choi[b], Bangho Shin[a], Hyeonil Kim[a], Suhyeon Kim[a], Soon Young Song[c], Hyoungtaek Kim[d], Min Chae Kim[a, d], Chan Hyeong Kim[a*]
[a]*Department of Nuclear Engineering, Hanyang University, Seoul, Korea*
[b]*J Crayton Pruitt Family Department of Biomedical Engineering, University of Florida, Gainesville, FL, USA*
[c]*Department of Radiology, Hanyang University Seoul Hospital, Seoul, Korea*
[d]*Radiation Safety Management Division, Korea Atomic Energy Research Institute, Daejeon, Korea*

[*]*Corresponding author: chkim@hanyang.ac.kr*

1. Introduction

In interventional radiology, radiologists continuously observe the radiographic image next to the patient, leading to relatively high radiation exposure. Indeed, the occupational dose to radiologists was reported to be the highest among the medical personnel [1]. To monitor occupational doses to radiologists, $H_p(10)$ is generally measured by the personal dosimeter worn under the lead apron and above the apron at the collar level [2]. However, large measurement uncertainties of personal dosimeters are inevitable [3] and even if we assume that the measurement is perfect, $H_p(10)$ can be largely different from effective dose for low-energy photons (<0.1 MeV) [4]. Furthermore, radiologists are reluctant to wear dosimeters due to inconveniences. These issues of incorrect and irregular use of dosimeters have been raised in the previous studies [5]. Considering the limitations of personal dosimeters, the International Commission of Radiological Protection (ICRP) recommended to develop a computational dose calculation system which does not require a physical dosimeter in *Publication* 139 [6]. In this context, a Monte Carlo dose calculation system is under development for interventional radiology, and as part of the work, in the present study, an experimental validation of the developed system was performed. For this, radiation doses were measured using thermoluminescence (TL) elements attached to a Rando phantom, and the measured dose were compared with the doses calculated by the developed Monte Carlo dose calculation system.

2. Material and Methods

Figure 1. Experiment setup in the Hanyang University Medical Center (HYUMC) angiography room.

The experiment was performed in the angiography room of Hanyang University Medical Center (HYUMC) equipped with an Allura Xper FD 20/20 (Philips, Netherlands) C-arm. To imitate the patient body, a 30 × 30 × 15 cm^3 solid water phantom was placed on the operating table, and the operating table was adjusted to align the centers of the solid water phantom and the beam. Next, an Alderson Rando torso phantom was placed at a typical position of the radiologist, on a supporting table to set the height of the Rando phantom as 175 cm. Then, three disk-type LiF:Mg,Cu,Si TL elements [7] having a diameter of 4.5 mm and thickness of 0.8 mm were attached to four sites of the torso phantom: forehead, right chest, left flank, and pelvis (see figure 1). In addition, three TL elements covered by the 10-mm-thick bolus material were attached to the left chest of the phantom to measure the $H_p(10)$, replacing the personal dosimeter; this is because the personal dosimeters are not generally calibrated using the same radiation qualities of diagnostic X-ray [8]. Note that the effect of the background radiation was minimized by annealing the TL elements with a dual-step thermal treatment [7] (300 ℃ for 10 min and 260 ℃ for 10 min) ~26 hours before the experiment. The X-ray beam was irradiated by an automatic exposure control in the continuous fluoroscopy mode. Table I shows the cases studied in the present study, which are typical C-arm projections in coronary angiography procedure [9].

Table I: Experimental cases for the C-arm projections

C-arm projections	PA	RAO 10°-CRA 40°	LAO 45°
Tube Voltage (kVp)	69	69	68
Tube Current (mA)	3.75	4.95	2.55
Time (sec)	1800	600	1202
Field-of-View	48 cm		
Source-to-Image Distance	100 cm		
Inherent filtration	2.5 mm Al		
Additional filtration	1.0 mm Al + 0.4 mm Cu		

The TL intensity of the irradiation elements was measured by using a Risø TL/OSL DA-20 (DTU Physics, Denmark). For each TL element, after measuring the TL intensity for dose received from the experiment, the TL intensity was additionally measured for a calibrated dose of 11.8 mGy irradiated by the built-in beta source ($^{90}Sr/^{90}Y$). The absorbed dose of each TL element (D_{LiF}) was then estimated using equation (1) [10].

$$D_{LiF} = 11.8 \times \frac{I_{LiF}}{I_{cal}} \times \frac{\sum_i \left(f_i \times (\mu_{en}/\rho)_{LiF/Air,i} \right)}{\sum_i \left(f_i \times R_{LiF,i} \right)} [\text{mGy}], \quad (1)$$

where I_{LiF} is the TL signal intensity of the LiF element for the dose irradiated in the experiment, I_{cal} is the TL signal intensity of the LiF element for the calibrated dose, f_i is the fraction of the ith energy bin in the spectra at each TL elements position theoretically calculated by the Geant4 Monte Carlo simulations [11], $(\mu_{en}/\rho)_{LiF/Air,i}$ is the ratio of mass-energy absorption coefficients of the LiF to air in the ith energy bin [12], and $R_{LiF,i}$ is the relative response of LiF to the reference field in the ith energy bin [13]. Note that in the present study, several factors mainly affecting the estimation of TL dose were considered to estimate the measurement uncertainty at a confidence level of approximately 95% (k = 2); that is, the uncertainty of reference irradiation (2.8%) provided by Korea Atomic Energy Research Institute (KAERI) was considered by including uncertainties such as the background radiation, reference instrument calibration factor, ionization current, time, temperature, and so on. In addition, the uncertainty in the calibration curve was estimated by considering the uncertainties in linearity (3%) and reproducibility (1.5%) provided by the manufacturer (ILJINRAD Co., Ltd., South Korea). The energy dependence uncertainty, on the other hand, was not included due to the difficulty in calculating the actual energy spectrum uncertainty [13]. The angular dependence was also not considered due to the small and thin structure of TL element [14].

For the calculation of the absorbed doses of TL elements, as well as their photon energy spectra, the experiment setup was simulated by Geant4. For this, a computational model of the Rando phantom was constructed by 3D scanning the phantom. Note that the inside of the Rando phantom was simply defined as ICRP tissue material without inner organ models assuming that their effect on the doses of TL elements is negligible. Three TL elements located at the five sites were modeled as a single circular patch with a diameter of 80 mm and a thickness of 0.8 mm, placed to cover all three elements by referring to the 3D scan data. For the elements at the left chest site, bolus material was additionally modeled as a circular patch with a diameter of 100 mm and a thickness of 10 mm. For the X-rays, a uniform beam profile was assumed with the energy spectra obtained from the SpekCalc program [15] considering tube voltage and filtration (3.5 mm Al + 0.4 mm Cu). The physics library of *G4EMLivemorePhysics* was used in Geant4 simulations and the relative error of the dose values was less than 5%.

3. Results and Discussion

The incident photons to the TL elements have energies of 10-60 keV, as shown in figure 2. It can be seen that photons incident on TL elements attached at higher level tend to have higher energies than those attached at lower level. This is due to the fact that

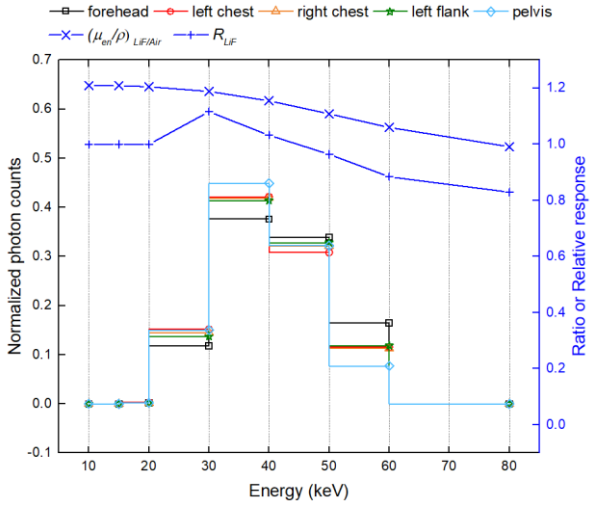

Figure 2. Incident photon energy spectra of the TL elements for attachment sites in PA projection, the ratio of mass-energy absorption coefficient of LiF to air, and the relative response of LiF.

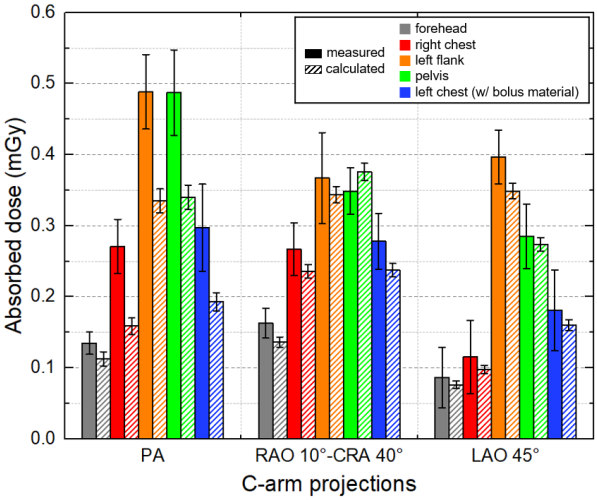

Figure 3. Comparison of measured and calculated absorbed dose rate of TL elements for C-arm projections. Error bars represent expanded uncertainty (k = 2).

photons with higher energies are likely to scatter in smaller angle, heading upward in this case where the initial beam is irradiated from the bottom of the solid water phantom. The correction factors, which are calculated by the ratio of the energy-weighted $(\mu_{en}/\rho)_{LiF/Air}$ and the energy-weighted R_{LiF}, were calculated to be 1.12-1.13 for all measurement sites in all projections. These results indicate that the shift in the energy spectrum according to the measurement sites dose not introduce a significant effect in correction factor.

Figure 3 compares the measured and calculated absorbed dose rates of TL elements for five measurement sites in PA, RAO 10°-CRA 40°, and LAO 45° projections. The measurement uncertainties were lower than 21% except for the low-dose level sites (i.e., forehead, right chest, left chest) in the LAO 45° projection. For RAO 10°-CRA 40° and LAO 45°

projections, in general, the Monte Carlo simulation slightly underestimates the doses to TL elements, but the differences were all within their uncertainties (k = 2). This small difference seems to be due to the fact that the support tables, rack, and floors are not modeled in Geant4 simulations. For the PA projection, however, the degree of the underestimation was much larger, showing the differences up to 42%. This discrepancy can be partly explained by the anode heel effect on the doses for PA projection. That is, when considering the experiment settings of this study, the beam profile may introduce ~1.2 times larger dose to cathode side, which is nearby the Rando phantom, than to the center of the beam [16]. Note that this effect is not significant in the other projections in which Rando phantom was generally irradiated by back-scattered photons. It was observed that the measured $H_p(10)$ (i.e., absorbed dose at left chest site) for the PA, RAO 10°-CRA 40°, and LAO 45° projections were 0.297, 0.278, and 0.181 mGy, respectively, showing that the simulated $H_p(10)$ of those projections were lower than the measured $H_p(10)$.

4. Conclusion

In the present study, for the experimental validation of the Monte Carlo dose calculation system for interventional radiology, the dose value measured using the TL elements and the dose value calculated by Monte Carlo simulation were compared. The results generally show that the Monte Carlo simulation slightly underestimates the doses to TL elements, but the differences were all within their uncertainties (k = 2) except for the PA projection. For the exception, the significant differences were observed due mainly to the anode heel effect. In the future work, the dose calculation system will be improved to estimate the radiologist doses in higher accuracy by additionally considering the beam profile and the effect by peripheral structures.

REFERENCES

[1] R. Padovani et al., International project on individual monitoring and radiation exposure levels in interventional cariology, Radiat. Prot. Dosim., 144(1-4), 2011.
[2] ICRP, Avoidance or radiation injuries from medical interventional procedures, ICRP Publication 85, Annal ICRP 30(2) (2000).
[3] P. Ambrosi and D.T. Bartlett, Dosimeter Characteristics and Service Performance Requirements, IAEA-TECDOC-1126, 1999.
[4] ICRP, Conversion Coefficients for Radiological Protection Quantities for External Radiation Exposures, ICRP Publication 116, Annal ICRP 40(2-5), 2010.
[5] IAEA, The Information System on Occupational Exposure in Medicine, Industry and Research (ISEMIR): Interventional Carioldogy, IEAE-TECDOC-1735, 2014.
[6] ICRP, Occupational Radiological Protection in Interventional Procedures, ICRP Publication 139, Annal ICRP 47(2), 2018.
[7] J. Lee, et al., Dual-step thermal treatment for the stability of glow curve structure and the TL sensitivity of the newly developed LiF:Mg,Cu,Si, Radiat. Meas., 42(4-5), 597-600, 2007.
[8] W. E. Muhogora et al., Energy response of LiF:Mg, Ti dosemeters to ISO 4037 and typical diagnostic x-ray beams in Tanzania, J. Radiol. Prot., 22(2), 175, 2002.
[9] A. Varghese et al., Radiation doses and estimated risk from angiographic projections during coronary angiography performed using novel flat detector, J. Appl. Clin. Med. Phys., 17(3), 443-441, 2019.
[10] Y. Choi et al., Reference dosimetry for inter-laboratory comparison on retrospective dosimetry techniques in realistic field irradiation experiment using ^{192}Ir, Nucl. Eng. Technol., 54, 2599-2605, 2022.
[11] J. Allison et al., Recent developments in Geant4, Nucl. Instrum. Methods Phys. Res. Sect. A., 835, 186–225, 2016.
[12] S. M. Seltzer, Calculation of photon mass energy-transfer and mass energy-absorption coefficients, Radiat. Res., 136(2), 147-170, 1993.
[13] Ž Knežević et al., Influence of dopants on the glow curve structure and energy dependence of LiF:Mg,Cu,Si detectors, Radiat. Meas., 46(3), 329-333, 2011.
[14] F. D.G. Rocha et al., Thin sintered Al_2O_3 pellets as thermoluminescent dosimeters for the therapeutic dose range, Appl. Radiat. Isot. 58(6), 719-722, 2003.
[15] G. Poludniowski et al., SpekCalc: a program to calculate photon spectra from tungsten anode x-ray tubes, Phys. Med. Biol., 54(19), 2009.
[16] H. Salleh et al., Anode-Cathode Position: How it influences the radiation risk to staff involved in fluoroscopy procedures, Adv. Mat. Res., 1087, 405-409, 2015.